ARL

US Army Research Laboratory

Anti-Jam GPS Antennas for Wearable Dismounted Soldier Navigation Systems

by Steven D Keller

NOTICES

Disclaimers

The findings in this report are not to be construed as an official Department of the Army position unless so designated by other authorized documents.

Citation of manufacturer's or trade names does not constitute an official endorsement or approval of the use thereof.

Destroy this report when it is no longer needed. Do not return it to the originator.

US Army Research Laboratory

Anti-Jam GPS Antennas for Wearable Dismounted Soldier Navigation Systems

by Steven D Keller
Sensors and Electron Devices Directorate, ARL

REPORT DOCUMENTATION PAGE

Form Approved
OMB No. 0704-0188

Public reporting burden for this collection of information is estimated to average 1 hour per response, including the time for reviewing instructions, searching existing data sources, gathering and maintaining the data needed, and completing and reviewing the collection information. Send comments regarding this burden estimate or any other aspect of this collection of information, including suggestions for reducing the burden, to Department of Defense, Washington Headquarters Services, Directorate for Information Operations and Reports (0704-0188), 1215 Jefferson Davis Highway, Suite 1204, Arlington, VA 22202-4302. Respondents should be aware that notwithstanding any other provision of law, no person shall be subject to any penalty for failing to comply with a collection of information if it does not display a currently valid OMB control number.
PLEASE DO NOT RETURN YOUR FORM TO THE ABOVE ADDRESS.

1. REPORT DATE *(DD-MM-YYYY)*	2. REPORT TYPE	3. DATES COVERED (From - To)
June 2016	Final	09/2014–09/2015

4. TITLE AND SUBTITLE	5a. CONTRACT NUMBER
Anti-Jam GPS Antennas for Wearable Dismounted Soldier Navigation Systems	
	5b. GRANT NUMBER
	5c. PROGRAM ELEMENT NUMBER
6. AUTHOR(S)	5d. PROJECT NUMBER
Steven D Keller	TPA # CE-SE-2014-09
	5e. TASK NUMBER
	5f. WORK UNIT NUMBER

7. PERFORMING ORGANIZATION NAME(S) AND ADDRESS(ES)	8. PERFORMING ORGANIZATION REPORT NUMBER
US Army Research Laboratory ATTN: RDRL-SER-M 2800 Powder Mill Road Adelphi, MD 20783-1138	ARL-TR-7670

9. SPONSORING/MONITORING AGENCY NAME(S) AND ADDRESS(ES)	10. SPONSOR/MONITOR'S ACRONYM(S)
CERDEC Command, Power and Integration	
	11. SPONSOR/MONITOR'S REPORT NUMBER(S)

12. DISTRIBUTION/AVAILABILITY STATEMENT

Approved for public release; distribution is unlimited.

13. SUPPLEMENTARY NOTES

14. ABSTRACT

Approaches for the design and fabrication of a wearable anti-jam global positioning system (GPS) antenna are explored to support accurate and uninterrupted position, navigation, and timing information for the dismounted Soldier. The state of the art for anti-jam GPS antenna technology is presented, including GPS antenna element and array designs, and algorithms for jammer mitigation, and the candidate technologies best fit for wearable anti-jam GPS systems are identified. Potential materials and fabrication methods that are most amenable to wearable anti-jam GPS antennas are explored, including textile-integrated embodiments and externally mounted/removable embodiments. Early measured results for a variety of textile-integrated carbon nanotube thread antennas are presented in order to explore the feasibility of applying bulk carbon nanotube materials to wearable anti-jam GPS antenna designs.

15. SUBJECT TERMS

antenna, wearable, anti-jam, GPS, carbon nanotube, radio frequency

16. SECURITY CLASSIFICATION OF:			17. LIMITATION OF ABSTRACT	18. NUMBER OF PAGES	19a. NAME OF RESPONSIBLE PERSON
					Steven D Keller
a. REPORT	b. ABSTRACT	c. THIS PAGE	UU	30	19b. TELEPHONE NUMBER (Include area code)
Unclassified	Unclassified	Unclassified			919-280-6670

Standard Form 298 (Rev. 8/98)
Prescribed by ANSI Std. Z39.18

Contents

List of Figures

1. Introduction

There is a critical need for the development of new Army navigation technologies that can provide accurate and uninterrupted position, navigation, and timing (PNT) information for the dismounted Soldier. An essential element in a navigation system is the global positioning system (GPS) receiver antenna, which must be designed to maintain a constant link with visible GPS satellites while providing robust protection against hostile jamming signals. Additionally, the antenna size, weight, power, and cost must be minimized, and it must be seamlessly integrated with specific platforms of interest without sacrificing performance. In collaboration with the Communications-Electronics Research, Development and Engineering Center (CERDEC) Command, Power & Integration Directorate (CP&I), wearable anti-jam GPS antenna designs and fabrication methods are being explored to support future dismounted Soldier navigation systems.

Initial efforts have focused on researching best approaches for design and fabrication of a wearable anti-jam GPS antenna. The results of this study will be summarized in this report. Section 2 will discuss the state of the art for anti-jam GPS antenna technology, including GPS antenna element and array designs and algorithms for jammer mitigation, and will identify the candidate technologies best fit for wearable anti-jam GPS systems. Section 3 will discuss potential materials and fabrication methods that are most amenable to wearable anti-jam GPS antennas, including textile-integrated embodiments and externally mounted/removable embodiments. Early measured results for a variety of textile-integrated carbon nanotube thread (CNT) antennas will be presented in order to explore the feasibility of applying bulk CNT materials to wearable anti-jam GPS antenna designs. Finally, Section 4 will present the path forward in this research.

2. Background/State of the Art for Anti-Jam Antennas

2.1 Motivation for Anti-Jam GPS Technology

GPS signals are transmitted from a set of orbiting satellites located at an altitude of ~20,200 km. Standard frequency bands for military use are the L1 (1575.42 MHz) and L2 (1,227.60 MHz) bands. Since the GPS signals are transmitted at only ~25 W (~27 dBW after the satellite antenna gain of 13 dB is considered), the received signal at a typical GPS receiver is significantly below the noise floor, on the order of –155 to –160 dBW. With such a low received signal, a hostile source with a 3 dBi gain antenna can effectively jam a GPS receiver located 100 km away with a less than 50-W transmitter.[1] Jammer to signal (J/S) level versus distance is shown

in Fig. 1 for a variety of jammer power levels (0.1- to 100-W EIRP). The red lines indicate the susceptibility threshold for a variety of acquisition methods, including the standard coarse acquisition (C/A) code, the P(Y) code that requires precise time to be known, and a GPS receiver that employs advanced signal processing correlation and filtering techniques to achieve signal recovery from the noise floor.
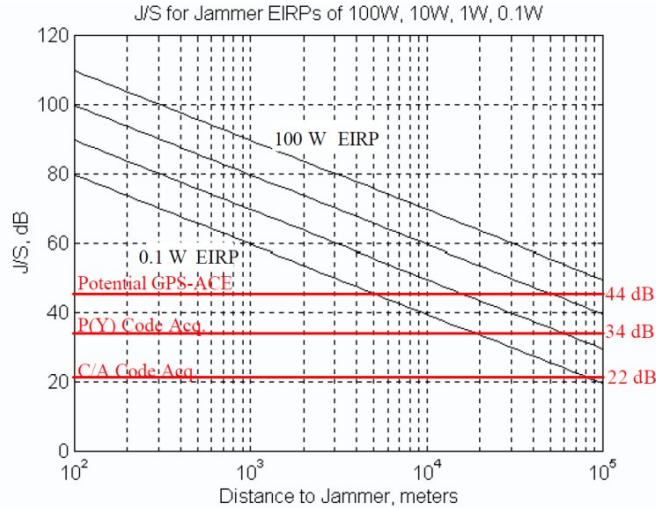

Fig. 1   Jammer to signal (J/S) level vs. distance for different jammer EIRP levels and susceptibility thresholds for different GPS signal acquisition methods[2]

Since the received GPS signals are below the noise floor of a typical GPS receiver, any signals detected above the noise floor can be classified as jammers/interferers and filtered accordingly. As a standard first step, fixed bandwidth front-end radio frequency (RF) filters are used to reject out-of-band jammers and general interference. For more robust filtering against continuous wave (CW) tone jammers, intermediate frequency adaptive notch filters can also be employed. These 2 techniques typically yield between 15 and 30 dB in jammer suppression with minimal effect on the GPS signal, itself, which is enough to mitigate the effects of moderate power jammers located at least 10 km away (using Fig. 1 as a reference). In order to deal with closer distance and/or high-power jammers, anti-jamming techniques beyond digital signal processing techniques and frequency-domain hardware filtering—such as spatial filtering that actively controls the radiation/reception pattern of the GPS antenna—must be employed.

2.2 Controlled Radiation Pattern Antenna

An excellent spatial filtering technique for anti-jam capabilities is the controlled radiation/reception pattern antenna (CRPA),[3] as shown in Fig. 2.
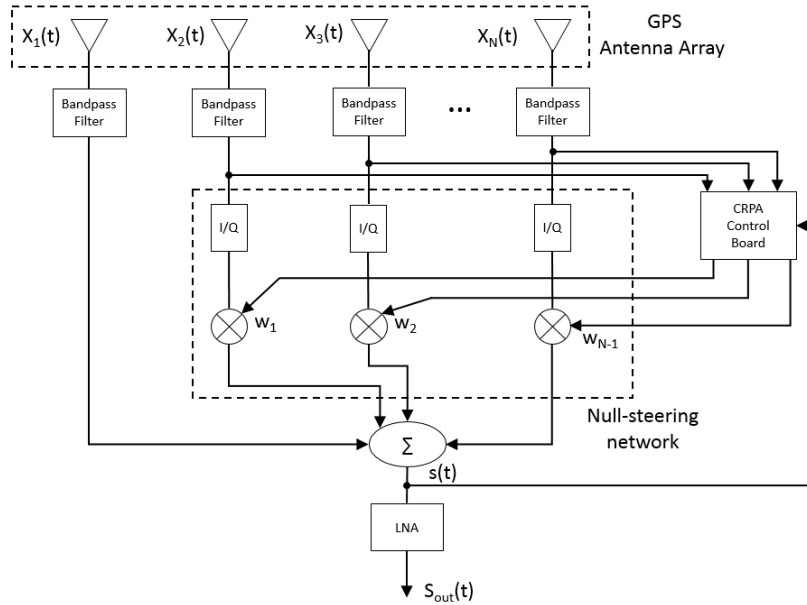
Fig. 2   Typical controlled radiation/reception pattern antenna (adapted from reference 1)

A standard CRPA leverages adaptive array theory[4] and comprises an adaptive array of GPS antennas, with the number of antenna array elements determined by the number of jamming signals that the system desires to protect against. An array of 'N' number of elements is capable of mitigating 'N-1' number of jamming signals. Typical vehicle-mounted military anti-jam GPS systems include a 7-element antenna array in order to mitigate the effects of 6 jamming signals. Each antenna in the array has dualband capabilities (L1 and L2 GPS bands), ~24 MHz bandwidth, realized gain of ~5 to 7 dBi, half power beamwidth (HPBW) of ~100 to 120°, and circular polarization. In addition to the GPS antenna array, a control board and null-steering network (phase shifters, attenuators, etc.) are needed to detect the jamming signal and adjust the array's radiation/reception pattern accordingly.

The CRPA operates by identifying the direction(s) of jamming signals in real-time, and then adjusting the amplitude and phase for each array element in order to minimize power reception in the direction(s) of the jamming signals while still maintaining reasonable reception in the directions of the visible satellites. The weight values for each array element are actively calculated by a basic optimization algorithm that attempts to minimize the jammer signal power at the combined received output signal, while keeping one of the array elements constant in order to guarantee the reception of valid GPS signals. The received RF signals from the array elements, $X1(t)$ to $XN(t)$, are mixed with these controlled amplitude and phase weights, $w1$ to $wN-1$, and summed to produce a radiation/reception pattern for the array with pattern nulls steered in the direction(s) of the jamming signals.

Figure 3 summarizes the GPS jammer problem space and the solution that a wearable CRPA anti-jam system can provide for the dismounted Soldier.
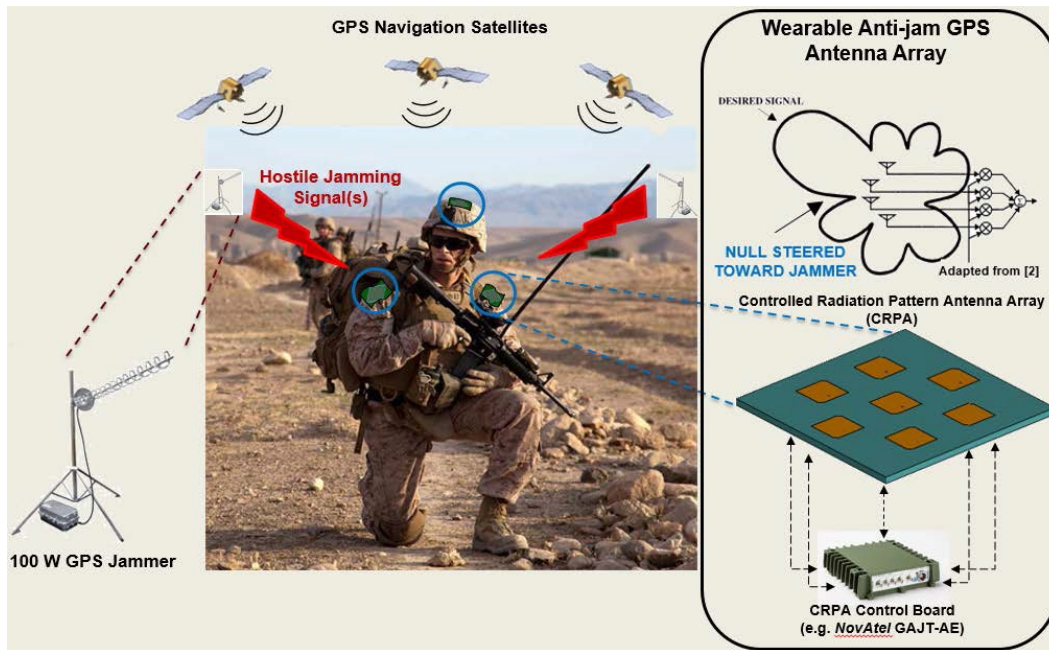
Fig. 3   **Cartoon overview of GPS jammer threat and CRPA anti-jam system**

This active null-steering technique can provide an additional 30–50 dB in jammer suppression, enabling the CRPA anti-jam GPS system to mitigate the effects of much closer and higher power jamming signals than standard GPS receivers. The benefit of this technique can be seen by reexamining the jammer-to-signal ratio versus distance-to-jammer plot, and overlaying the suppression contributions of frontend filters, DSP, and active null-steering, as shown in Fig. 4.
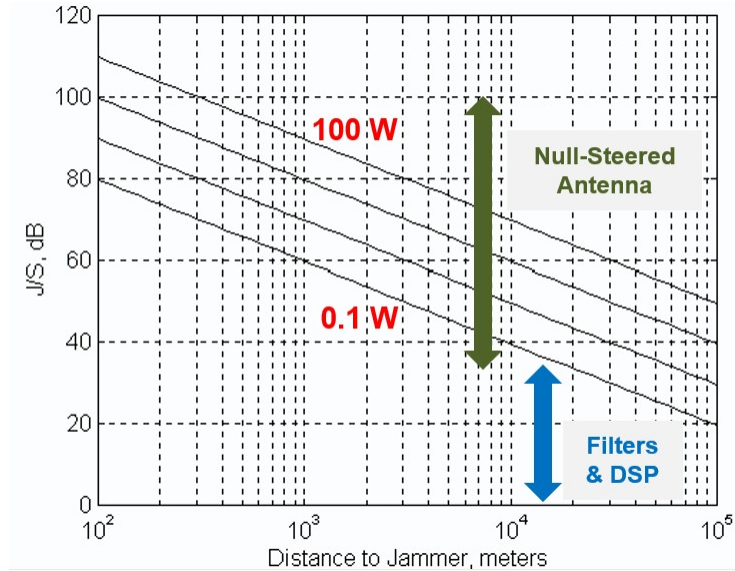
Fig. 4   Jammer suppression capabilities overlaid on jammer-to-signal vs. distance to jammer plot (adapted from reference 2)

Some of the research on CRPAs over the past 2 decades has focused on improving upon the basic null-steering algorithm previously described. A space-time adaptive beamformer has been proposed to maintain degrees of freedom in the presence of multiple jammers when near-field multipath signals are present.[5] CRPA variations that employ dual linear-polarized GPS antenna elements to exploit polarization diversity have been explored in order to increase the flexibility of the optimization criteria used in the null-steering algorithm and increase the number of broadband jammers that can be mitigated with a fixed number of array elements.[6–8] The application of a variety of direction-of-arrival algorithms to a GPS CRPA system, including multiple signal classification (MUSIC) and standard and conjugated estimation of signal parameters via rotational invariance techniques (ESPRIT and C-ESPRIT), have also been explored and evaluated.[9]

More recent research has begun to explore null-steering algorithms and adaptive array layouts for conformal[10] and nonplanar[11] adaptive arrays in order to extend the application of GPS CRPAs to nonplanar platforms such as small aircraft fuselages. As part of this program, the results of this nonplanar CRPA research will be leveraged and expanded upon in order to develop novel null-steering algorithms and theoretical models of distributed adaptive subarrays. These algorithms and models will be critical to the development of a wearable GPS CRPA that is strategically distributed on the human body to maximize GPS signal reception and optimize anti-jam capabilities.

We will consider 2 different topologies for the nonplanar adaptive array. In the first case, individual antenna elements will be assumed to lie at different points on the

Soldier's body. In the second case, planar subarrays that are fewer in number will be distributed on the Soldier's body. The former demands more strategic locations where the elements can be placed and offers more control, while the latter may be the only option available when the Soldier is in a crouching position. In both cases, optimum receive weights that will extract the desired source in the presence of strong jammers will have to be determined either by maximizing the signal-to-interference-plus-noise-ratio (SINR), or by minimizing the mean square error between the actual and desired output.[11,35,36] The relative advantages of these topologies in their ability to null out the interferers in a dynamic environment will be studied and developed through this program.

2.3 Antenna Element and Array Design for Anti-Jam GPS Systems

The antenna element design for a CRPA is also of critical importance, particularly for a wearable anti-jam GPS system with limited real estate and a need for conformability and flexibility. Antennas for vehicle-mounted GPS systems are typically planar dualband designs, such as the stacked patch antenna,[12] which satisfies all RF requirements for a GPS antenna in a reasonably compact, planar design. Basic stacked patch GPS antennas are fabricated on a low-loss, low-dielectric constant rigid substrate, such as RT Duroid 5870, and are either notched at 2 of the patch corners or possess 2 feedlines to achieve circular polarization. Early 7-element CRPA designs have employed these antennas as elements in a circular array layout, with array elements placed at approximately half wavelength (λ/2) spacing to minimize grating lobes and mutual coupling. The center element serves as the reference antenna for the null-steering algorithm. A first-cut model of a pin-fed patch CRPA, modeled by ARL in FEKO, is shown in Fig. 5.
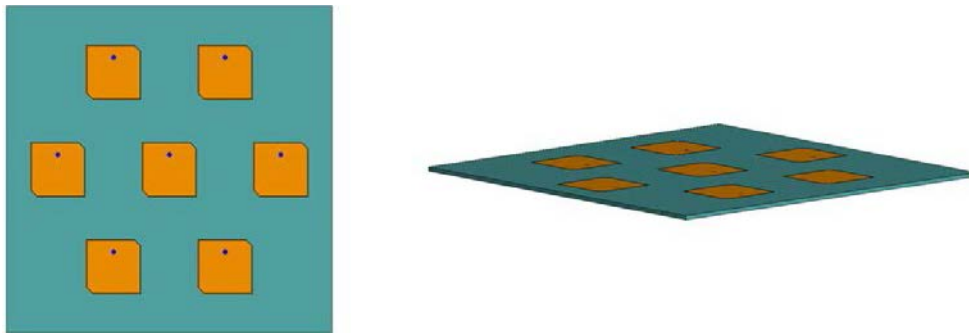

Fig. 5   Seven-element CRPA modeled in FEKO

The diameter of a 7-element CRPA is ~14–16 inches when the antenna elements are spaced approximately λ/2 apart and no antenna size reduction techniques are employed. Variations on this design have been researched in recent years for both

commercial and military vehicle-mounted GPS systems, with particular emphasis being placed on reducing the array size while maintaining reasonable realized gain and bandwidth. For a vehicle-based, Army anti-jam GPS antenna, the Novatel GAJT-700M/L CRPA is currently being considered, as shown in Fig. 6.

Fig. 6   A basic 7-element CRPA (right) compared with a size-reduced CRPA (left)[13]

The dimensions for this antenna are $11.5 \times 11.5 \times 4.7$ inches, making it too large for a wearable system. Using strictly a high-dielectric constant substrate and maintaining half-wavelength element spacing, a 4-element single band (L1) patch antenna CRPA has been realized with a 6-inch diameter size.[2] This design is compact but only singleband and would be considerably larger if it were redesigned to accommodate the L2 GPS frequency band (1,227.60 MHz). By employing a dielectric superstrate as a lens to maintain a half-cycle phase relationship for received signals across all elements in an array spaced less than $\lambda/2$ apart, the diameter of a 7-element L1/L2 band stacked patch antenna CRPA has been reduced to ~5.3 in.[14] While very compact in the horizontal plane, this CRPA accomplishes its diameter size reduction by increasing the height of the array from less than 1 inch to over 5 inches and by including a high dielectric constant superstrate lens that will add considerable weight to the array. For a wearable anti-jam GPS system, a 7-element CRPA design that minimizes diameter, thickness, and weight, while maintaining high RF efficiency, will be needed.

A dualband stacked patch antenna element at less than $\lambda/8$ x $\lambda/8$ in size has been developed for GPS applications at L1, L2, and the more recent L5 band (1176.45 MHz).[15] This design mainly relies on very high dielectric constant substrates (?r = 15 for top layer, ?r = 30 for bottom layer). A further development of this design introduced an integrated 0° to 90° branch-line hybrid, single-input feed to simplify the original dual-input quadrature phase feeding mechanism.[16] When this design was examined in array format, the integration of the branch-line hybrid feed directly under the stacked patch antenna was found to significantly increase mutual coupling at close array spacing ($<\lambda/6$).[17] By enlarging the

branch-line hybrid feed to be located outside of the high dielectric constant stacked patch region of the antenna, a significant reduction in mutual coupling was achieved. A full 7-element L1/L2/L5 band CRPA that includes this design was explored in Zhou et al.[18] The overall size of this CRPA (not including the null-steering control unit) was ~4.5 inches in diameter and ~0.7 inches in height. While functionality at the L5 band will not be needed for Army applications at this time, a variation on this stacked patch antenna design that can be textile-integrated or fabricated on a flexible substrate may be suitable for development of a wearable Army anti-jam GPS CRPA. In Zhou et al.,[19] the GPS array element was further miniaturized to measure 1-inch diameter by incorporating slots on the patch, as shown in Fig. 7a. Design for a 4-element L1/L2-band array on a circular aperture with a 3.5-inch diameter was shown. Apart from stacked-patch configurations, a single-layer microstrip patch antenna—illustrated in Fig. 7b—was shown to have broadband matching as well as axial ratio bandwidths.[20] A possible single-layer patch element for L1/L2-dualband operation with circular polarization in both bands will also be considered. A focus for this program will be on adapting such a design to be realizable with materials and fabrication techniques that are most suitable for wearable (textile-integrated and/or externally-mounted) antennas. This will be discussed further in the following section.

(a) (b)
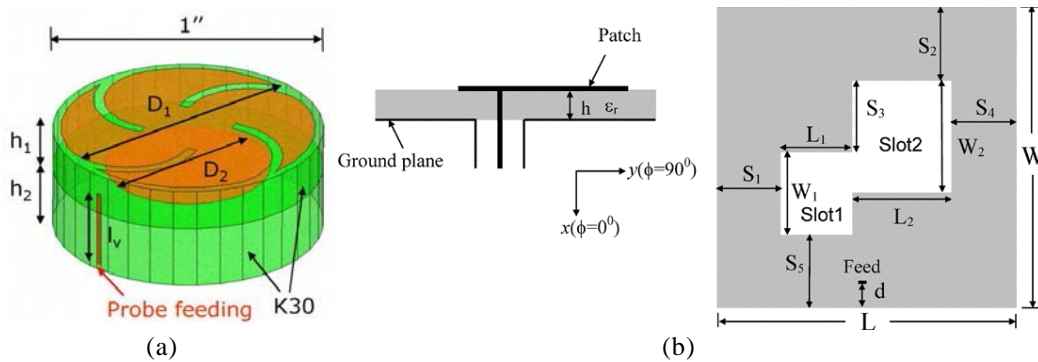
Fig. 7   Modern GPS antenna elements: a) dual L1/L2-band element[19] and b) broadband, circularly polarized patch antenna[20]

3.   Materials and Fabrication Methods for Wearable Anti-Jam GPS Antennas

A variety of design and fabrication possibilities exist for development of wearable anti-jam GPS antennas. Most notably, the choice of whether the CRPA will be externally worn and removable or whether it will be fully textile-integrated, will lead to the use of distinct antenna designs, materials, and fabrication methods. This section will discuss potential materials and fabrication methods for each of these versions of a wearable anti-jam GPS antenna.

3.1 Textile-Integrated Antennas

The development of a textile-integrated anti-jam GPS antenna presents a variety of material and fabrication challenges. Textile-integrated antennas can be fabricated with a variety of conductive materials, including thin metallic wires, textile fibers coated with conductive nanoparticles, and fibers with metallic cores. While these materials exhibit high conductivity and are relatively simple to fabricate and integrate into a textile, they fail to endure significant "wear-and-tear" due to corrosion and lack of durability. This limits their placement to areas on the body that see minimal flexing and bending and requires significant steps to prevent performance-hindering corrosive damage. The application of bulk carbon nanotube (CNT) thread as a lightweight, durable radiator has emerged as a promising solution to this challenge due to its inherent moderate conductivity (104–106 S/m) and unique physical properties compared to traditional conductive materials. These include high tensile strength (measured >1 GPa), corrosion resistance, extremely low weight, and excellent work hardening, with the ability to withstand repetitive flexing and bending without developing performance-degrading microcracks.[21–23]

While extremely low-efficiency antennas result when individual CNTs are employed as RF radiators due to the dominant kinetic inductance that each nanoscale CNT contributes to the antenna's high input impedance,[24,25] it has been found through analysis[26,27] and measurement[28] that it is possible to mitigate this high reactance by fabricating macroscale CNT bundles or threads. CNT bundles can exhibit radiation efficiencies orders of magnitude higher than those of individual CNTs[29] and improved efficiency as the nanotube density within the bundle is increased.[30]

Emerging fabrication techniques have made realizable the synthesis of large-scale CNT bundle structures such as threads, ribbons, and sheets. By synthesizing large-scale multiwall carbon nanotube (MWNT) bundle structures in the form of threads,[31] and then by applying these bulk CNT materials to produce textile-integrated RF antenna designs, it should be possible to fabricate extremely low-profile wearable anti-jam GPS antennas with significantly enhanced flexibility and durability when compared to antennas fabricated with traditional textile-based conductive materials.

A diagram of the CNT thread fabrication process is shown in Fig. 8. The fabrication process begins with the synthesis of a unique density and length of vertically aligned CNTs into a spinnable array, which typically contains double, triple, and multiwall CNTs. This spinnable array is used to assemble continuous CNT threads, yarns, and fibers by simply grabbing one spot in the array with forceps, then dragging and twisting in a manner similar to that used in the fabrication of a silk

fiber from its cocoon.[32,33] Due to the unique density and length of the CNTs within the array, there are enough contact points that enable CNT thread assembly by a simple Van der Waals interaction between neighboring CNTs. In order to fabricate a spinnable CNT array, a thin catalyst of 2-nm iron alloy is deposited on 5-nm Al_2O_3 that has a 4-inch silicon wafer as support. The as-prepared catalyst is introduced into a chemical vapor deposition (CVD) reactor at 750 °C, where CNTs grow under a stream of an argon, C_2H_4, H2, and H_2O mixture.[34] The as-grown CNT array has a density of 0.03 gm/cm3 and an average CNT length of 500 µm. The final thread diameter of a 1-ply (single ply) thread is controlled by the width of a spinnable CNT array, where a 0.5-inch width array typically produces 20- to 25-µm-diameter CNT thread. By adding a weaving process into the overall spinning process with multiple spools of 1-ply thread, a variety of larger-ply CNT rope may be fabricated, including 3-ply CNT rope and a 3×3-ply CNT rope (three 3-ply CNT ropes spun together).
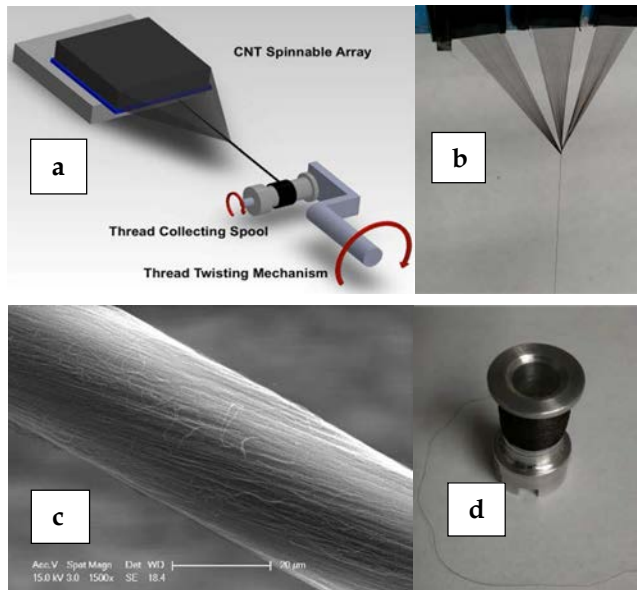

Fig. 8   Manufacturing steps in CNT thread formation: a) schematic of spinning CNT thread from CNT array, b) assembling CNT thread from 3 CNT arrays, c) scanning electron microscope image of pristine CNT thread, and d) CNT thread coiled on a bobbin

The application of this emerging material to produce a textile-integrated, anti-jam GPS antenna will require 3 things: 1) a material conductivity high enough to ensure a reasonable realized gain for the antenna with minimal RF losses, 2) a reliable fabrication method to sew the CNT thread into an Army-relevant textile (NyCo Ripstop, CORDURA, etc.) and electrically connect it to an RF input port such as an SMA connector, and 3) an antenna design that is realizable using a textile-based fabrication method.

As a first step in investigating CNT thread as a viable material for the fabrication of a wearable anti-jam GPS antenna, a textile-integrated CNT thread bowtie antenna has been fabricated and measured in collaboration with the University of Cincinnati. A single 45-µm-diameter CNT thread was fabricated and stitched into 1,000-denier coated Cordura nylon fabric using a Brother 40e sewing machine, as shown in Fig. 9. This particular sewing machine was used due to its versatility, as it has low, medium, and high automatic sewing speeds, and 50 types of sewing styles. The jam-resistant lower bobbin facilitates continuous stitching without thread jamming.
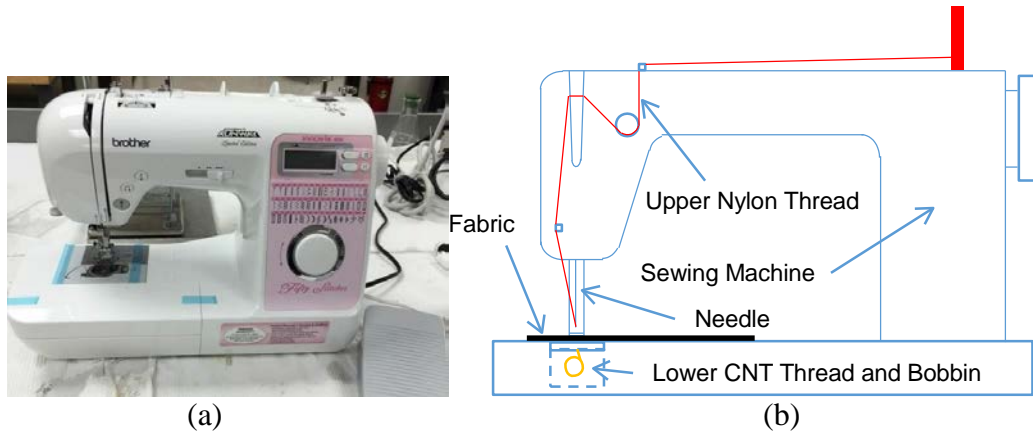

Fabric
Upper Nylon Thread
Sewing Machine
Needle
Lower CNT Thread and Bobbin

(a)   (b)

Fig. 9   Sewing machine: a) Brother 40e sewing machine and b) schematic of sewing

The CNT thread was densified with N-Methyl-2-pyrrolidone prior to textile integration in order to increase its strength. Densified CNT thread and glossy smooth nylon thread were used in the lower and upper bobbins of the sewing machine, respectively, to fabricate the textile-integrated bowtie antenna. Nylon thread was blended with the CNT thread during the fabrication process due to the CNT thread not being able to withstand the loading force of the sewing machine when placed in the upper bobbin, which generally exerts a higher load than the lower bobbin in the sewing process. CNT thread has greater tensile strength than nylon thread or copper wire. Thus, when integrated into a textile, it is able to withstand much higher stretching and bending loads and has much higher resistance to the formation of bending/flexing-induced microcracks than metallic wires or metal-coated nylon threads. However, the breaking load and the maximum loading capacity for nylon thread is higher than CNT thread because of the difference in the diameters of both fibrous materials. The diameter of the nylon thread is ~120 µm and its tensile strength is 75 MPa with a maximum loading capacity of 0.85 N. The CNT thread with 45-µm diameter has ~480 MPa tensile strength and a maximum loading capacity of 0.76 N. Since the nylon thread has higher loading capacity than CNT thread, it was used in the upper bobbin to form a blended final conductive

11

pattern within the Cordura textile substrate. As the upper nylon thread penetrated through the fabric sample and created a knot with the lower CNT thread in one sewing cycle, the CNT thread was pulled out from the lower bobbin and stitched into the fabric sample. The tightness of both upper and lower thread was set as medium so that the friction force of the CNT thread and nylon thread was balanced.

Research in future years will focus on increasing the stable diameter of the CNT thread in order to increase its loading capacity to the point where no nylon thread-blending is necessary, and CNT thread can be used for both the upper and lower bobbins in the textile-integrated antenna fabrication process.

The textile-integrated bowtie antenna was fabricated by sewing CNT thread into a 1,000-denier Cordura fabric substrate to form a trapezoidal area of ~10 × 2 × 20 mm using multiple zigzag patterns with a width of 3 mm and pitch of 0.3 mm. Due to the need to blend the CNT thread with nylon thread, as previously described, the CNT thread was sewn into the top surface of the CORDURA fabric and the nylon thread was sewn into the bottom surface. In order to facilitate soldering the CNT material to a coaxial connector, a rectangular section of CNT sheet material was stitched manually to the feedpoint of each bowtie leg with a single CNT thread, as shown in Fig. 10.

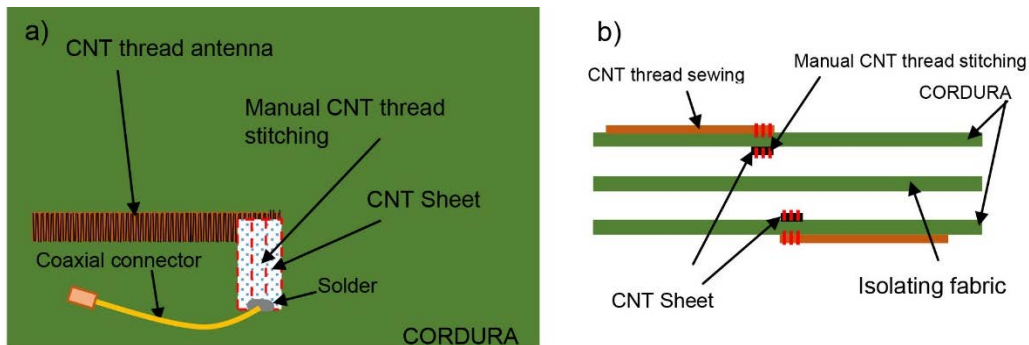**Fig. 10   Schematic of textile-integrated CNT thread antenna a) top view and b) side view**

The CNT sheet material was prefunctionalized by plasma treatment for enhanced solderability. The other end of each section of CNT sheet material was soldered to the inner or outer conductor of an SMA coaxial connector. The fully fabricated textile-integrated CNT thread bowtie antenna is shown in Fig. 11.

Fig. 11   CNT thread bowtie antenna fabricated on 1,000-denier CORDURA fabric

A model of this textile-integrated CNT thread bowtie antenna was simulated using the FEKO full-wave electromagnetic simulation software, as shown in Fig. 12. The CORDURA fabric substrate was approximated as a thin slab with $\varepsilon_r = 1.9$, $\mu_r = 1$, and $\tan(\delta) = 0.0098$. The CNT thread was simplified as a basic conductive sheet with sig = 3e5 S/m, based on recent conductivity measurements of the CNT thread.
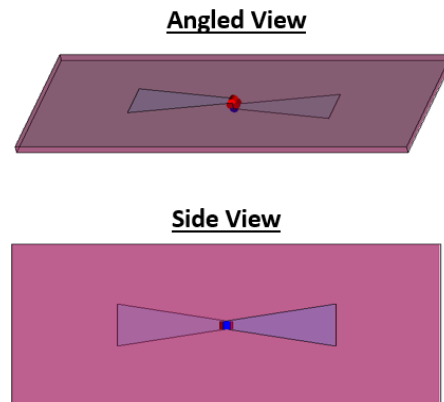
Fig. 12   FEKO model of CNT thread bowtie antenna

The simulated and measured reflection coefficient (S_{11}) data is shown in Fig. 13. The measured resonant frequency (2.6 GHz) agrees reasonably well with the simulated resonant frequency (2.63 GHz), shifted ~1% lower than its predicted value. This shift is likely due to fabrication tolerances and minor variations in the dielectric constant of the fabric substrate. The measured reflection coefficient is generally 6–8 dB higher than what the simulations predicted, indicating higher input impedance mismatch. This difference is expected since the FEKO model significantly simplified the CNT thread section of the bowtie antenna, modeled as a cohesive conductive sheet instead of discrete CNT threads stitched into the fabric

and overlapping each other to form a conductive mesh. This discrete conductive mesh likely contributes a significant amount of resistive loss to the antenna. Additionally, the model did not include important physical and quantum-level electrical effects that impact the resistance and reactance of the individual CNT threads, including quantum capacitance and kinetic inductance, and the finite lengths of the CNTs within the thread. As a result of these higher reflection losses, the measured $S_{11} < -10$-dB bandwidth is only 3% versus the simulated estimate of 15%.
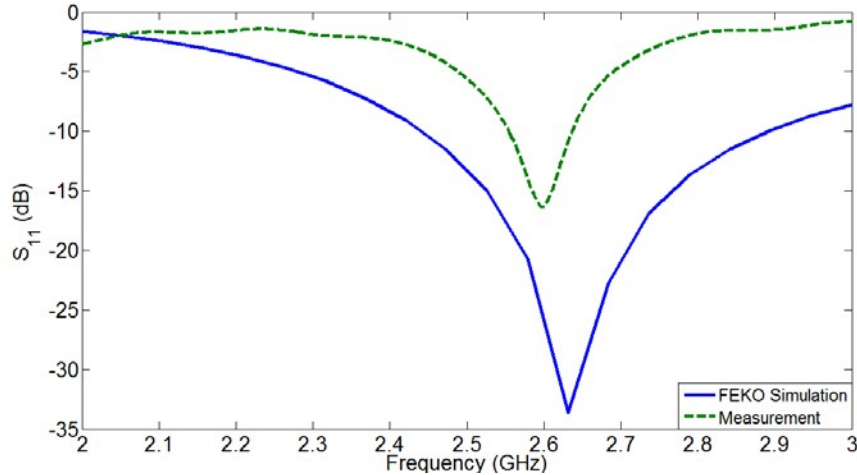

Fig. 13   Reflection coefficient for CNT thread bowtie antenna

The simulated and measured E-plane and H-plane radiation pattern data at resonance is shown in Figs. 14 and 15, respectively. The realized gain is ~5–10 dB lower than the simulated estimate, indicating significant RF losses in the material that were not accounted for in the simulation model. As mentioned previously, some of this loss may be attributable to physical and quantum-level electrical effects that impact the resistance and reactance of the individual CNT threads and to the discrete meshed structure of the stitched CNT thread antenna. Thus, the overall conductivity of the material, when taken as a whole instead of considering each discrete thread, may be significantly less than the 3e5 S/m that was used for the simulation. Additionally, both patterns stray from the expected performance of a standard bowtie antenna, which should yield a "doughnut"-shaped pattern similar to a dipole antenna. This indicates that the current flow along the conductive section of the antenna is not uniform and is anisotropic compared with a cohesive conductive sheet or mesh. Since electrons generally only flow axially along the CNT walls within the thread, the sections of the stitched CNT thread mesh that are orthogonal to the length of the bowtie may significantly disrupt the current flow and lead to radiation pattern distortions.
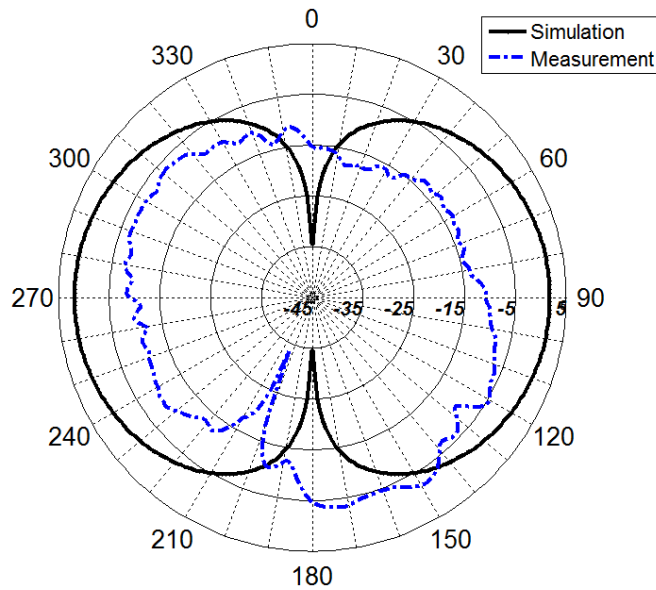
Fig. 14   E-plane radiation pattern (f = 2.6 GHz) for CNT thread bowtie antenna
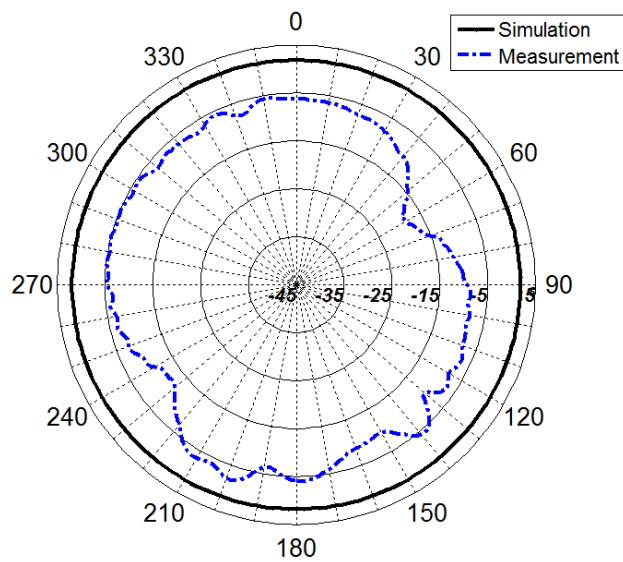
Fig. 15   H-plane radiation pattern (f = 2.6 GHz) for CNT thread bowtie antenna

The measured data for this textile-integrated CNT thread bowtie antenna indicates that many improvements must be made to the fabrication process and the CNT material, itself, in order to serve as a viable candidate for a textile-integrated anti-jam GPS antenna. Specifically, methods must be explored to yield a much more cohesive, isotropic conductivity along the stitched CNT thread mesh area, which will prove challenging due to the inherent anisotropic conductivity of the individual CNT threads. Improvements to the thread conductivity and reduction of reactance

losses in the material will likely reduce RF losses in the antenna and subsequently improve the realized gain.

3.2 Flexible Polymer-Based Antennas

An alternative to a fully textile-integrated antenna is one that is fabricated onto a flexible substrate and then placed externally onto the Soldier uniform by means of a durable, reusable adhesive, such as Velcro. A flexible substrate is essential for such an antenna to ensure that it can conform to a specific area of the body without impeding the mobility of the Soldier. Additionally, the substrate must possess high electric permittivity ($?_r$) and/or permeability (μ_r) in order to facilitate size reduction techniques needed to fit the L-band CRPA on the human body (as described in Section 2.3).

The development of flexible, high-permeability polymer materials for electrically small CRPA designs may be possible by exploring of a variety of classes of lightweight flexible materials, including conjugated polymers and graphene inserts, which can be modified to induce higher magnetic permeability than that of the host material. The properties of the host material may be modified by doping with high-spin metal cations, either alone or bonded to magnetic organometallic complexes. The determination of the metal-based dopant is guided by quantum chemistry calculations that consider a broad range of metal-ligand complexes with different chemistries and structures. Prior quantum chemistry simulations conducted by ARL have yielded results on structure-property relationships of the organometallic complexes, such as spin state and magnetic permeability, that facilitate the determined of ideal dopants for graphene and polymers of interest.[37] By leveraging these results, a class of conjugated polymers complexed with high-spin metal cations or organometallics can be synthesized by chemical methods such that they possess both electrical and ferromagnetic properties.

Recent ARL research has demonstrated metamaterial/metasurface blocks with high permeability. The unit cell that comprises such material can be arranged in periodic or random patterns that are printed on dielectric support layers. It may be possible to apply this method for producing high-permeability material by embedding graphene into specialized flexible polymer materials to manufacture very lightweight, flexible ferromagnetic substrates. This approach will involve thousands of graphene layers arranged in periodic lattice for anisotropic behavior or at random for isotropic behavior. An example of such a high permeability metamaterial substrate is shown in Fig. 16.

Fig. 16   High-permeability metamaterial substrate using patterned metallic layers

Patterning graphene and transferring it to a flexible polymer host material constitutes a major fabrication challenge. The present state of the art uses layered sheets of ferrites, realizing 5× weight reduction and keeping the magnetic loss tangent less than 0.1 up to frequencies of 500 MHz. Recent technologies have been developed to demonstrate methods of graphene patterning, printing, and transferring to polymers. These scientific advancements will be explored through collaboration in order to realize lightweight, flexible ferromagnetic substrates for the design of compact wearable anti-jam GPS antennas.

4.   Conclusion

The development of a wearable anti-jam GPS antenna will require research in a variety of distinct areas, including array null-steering algorithm development, flexible substrate and conductive thread fabrication, and wearable GPS antenna element and array design. ARL has specific expertise suitable for accomplishing the design, simulation, fabrication, and testing of wearable GPS antenna element and arrays. For the CRPA null-steering algorithm development and flexible substrate/conductive thread fabrication research, we will pursue specific university partnerships that offer expertise in these areas, including development of the null-steering algorithms described in Section 2, adapting them for application in a body-distributed CRPA system, and developing high μ_r and ϵ_r flexible polymer substrates to facilitate fabrication of electrically small wearable CRPA designs. Partnerships will also be established to research high conductivity carbon nanotube threads and the fabrication of textile-integrated GPS antenna designs.

5.   References

1. Mingjie D, Xinjian P, Fang Y, Jianghong L. Research on the technology of adaptive nulling antenna used in anti-jam GPS. Proc. of 2001 CIE International Conference on Radar; 2001 Oct. p. 1178–1181.

2. Brown A, Reynolds D, Tseng H-W. Miniaturized GPS antenna array technology. Proc. of ION 55th Annual Meeting; 1999 June.

3. Gordon LG, Eilts HS, Volpi JP, inventors. Texas Instruments Incorporated, assignee. Directed reception pattern antenna. United States patent US 5410321A, Filed Sept 29, 1993. Issued Apr. 25, 1995.

4. Widrow G, Mantey PE, Grifiths LJ, Goode BB. Adaptive antenna systems. Proc. of IEEE. 1967;55(12):2143–2159.

5. Hatke GF. Adaptive array processing for wideband nulling in GPS systems. Proc. of 32nd Asilomar Conference on Signals, Systems & Computers. 1998;2:1332–1336.

6. Trinkle M, Cheuk W-C. Null-steering GPS dual-polarized antenna arrays. Proc. of 6th International Symposium on Satellite Navigation Technology; 2003 July.

7. Fante R, Vaccaro J. Evaluation of adaptive space-time polarization cancellation of broadband interference. Proc. of 2002 IEEE Precision Location & Navigation Symposium; 2002. p. 1–3.

8. Ngai EC, Blejer DJ, Tri P, Herd J. Anti-jam performance of small GPS polarimetric arrays. Proc. of 2002 IEEE Antennas and Propagation Society International Symposium. 2002;2:128–131.

9. Kundu A, Ghosh S. Development of smart antenna array signal processing algorithm for anti-jam GPS receiver. Proc. of 2008 Progress in Electromagnetics Research Symposium; 2008 Mar. p. 125–131.

10. Knott P, Löcker C. Antenna element design for a conformal antenna array demonstrator. Proc. of 2011 IEEE Aerospace Conference; 2011 Mar.

11. Gupta IJ, Lee T-H, Griffith KA, Slick CD, Reddy CJ, Bailey MC, DeCarlo D. Non-planar adaptive antenna arrays for GPS receivers. IEEE Antennas and Propagation Magazine. 2010;52(5):35–51.

12. Long SA, Walton MD. A dual-frequency stacked circular-disc antenna. IEEE Transactions on Antennas and Propagation. 1979;AP-27(2):270–273.

13. Brown A, Morley D. Test results of a 7-element small controlled reception pattern antenna. Proc. of 2001 ION GPS; 2001 Sep.

14. Ly H, Eyring P, Traum E, Tseng H-W, Stolk K, Kurtz R, Brown A, Nathans D, Wong E. Design, simulation, and testing of a miniaturized GPS dual-frequency (L1/L2) antenna array. Proc. of 2002 ION GPS; 2002 Sep.

15. Zhou Y, Chen C-C, Volakis JL. Dual band proximity-fed stacked patch antenna for tri-band GPS applications. IEEE Transactions on Antennas and Propagation. 2007;55(1):220–223.

16. Zhou Y, Chen C-C, Volakis JL. Tri-band miniature GPS array with a single-fed CP antenna element. Proc. of 2007 IEEE Antennas and Propagation Society International Symposium; 2007 June. p. 3049–3052.

17. Zhou Y, Chen C-C, Volakis JL. Single-fed circularly polarized antenna element with reduced coupling for GPS arrays. IEEE Transactions on Antennas and Propagation. 2008;56(5):1469–1472.

18. Zhou Y, Chen C-C, Volakis JL. A single-fed element antenna for tri-band anti-jamming GPS arrays. Proc. of 2008 IEEE Antennas and Propagation Society International Symposium; 2008 July. p. 1–4.

19. Zhou Y, Chen C-C, Volakis JL. A compact 4-element dual-band GPS array. Proc. of 2009 IEEE Antennas and Propagation Society International Symposium; 2009. p. 1–4.

20. Ali M, Yang G, Dougal R. A new circularly polarized rectenna for wireless power transmission and data communication. IEEE Antennas and Wireless Propagation Letters. 2005;4:205–208.

21. Kang I, et. al. Introduction to carbon nanotube and nanofiber smart materials. Composites Part B: Engineering. 2006;37(6):382–394.

22. White CT, Todorov TN. Carbon nanotubes as long ballistic conductors. Nature. 1998;393:240–242.

23. Koziol K, Vilatela J, Moisala A, Motta M, Cunniff P, Sennett M, Windle A. High-performance carbon nanotube fiber. Science. 2007;318(5858):1892–1895.

24. Burke PJ, Li S, Yu Z. Quantitative theory of nanowire and nanotube antenna performance. IEEE Transactions on Nanotechnology. 2006;5(4):314–334.

25. Hanson GW. Radiation efficiency of nano-radius dipole antennas in the microwave and far-infrared regimes. IEEE Antennas and Propagation Magazine. 2008;50(3):66–77.

26. Salahuddin S, Lundstrom M, Datta S. Transport effects on signal propagation in quantum wires. IEEE Trans Elect Dev. 2005;52(8):1734–1742.

27. Raychowdhury A, Roy K. Modeling of metallic carbon-nanotube interconnects for circuit simulations and a comparison with Cu interconnects for scaled technologies. IEEE Transactions on Computer-Aided Design. 2006;25(1):58–65.

28. Plombon JJ, O'Brien KP, Gstrein F, Dubin VM. High-frequency electrical properties of individual and bundled carbon nanotubes. Applied Physics Letters. 2007;90.

29. Huang Y, Yin W-Y, Liu QH. Performance prediction of carbon nanotube bundle dipole antennas. IEEE Transactions on Nanotechnology. 2008;7(3):331–337.

30. Choi S, Sarabandi K. Performance assessment of bundled carbon nanotube for antenna applications at terahertz frequencies and higher. IEEE Transactions on Antennas and Propogation. 2011;59(3):802–809.

31. Mast D. The future of carbon nanotubes in wireless applications. Antenna Systems/Short-Range Wireless Conference; 2009 Sep.

32. Zhang MK, Atkinson K, Baughmann R. Multifunctional carbon nanotube yarns by downsizing an ancient technology. Science. 2004;306:1358–1361.

33. Jiang K, Li Q, Fan S. Spinning continuous carbon nanotube yarns. Nature. 2002;419:801.

34. Jayasinghe C, Supriya C, Schulz M, Shanov V. Spinning yarn from long carbon nanotube arrays. Journal of Materials Research. 2011;26:645–651.

35. Lambert JR, Balanis CA, DeCarlo D. Spherical cap adaptive antennas for GPS. IEEE Transactions on Antennas and Propagation. 2010;57(2):406–413.

36. Fante RL, Vaccaro JJ. Wideband cancellation of interference in a GPS receive array. IEEE Transactions on Aerospace and Electronic Systems. 2000;36(2):549–564.

37. Williams KS, Rinderspacher BC. High-permeability magnetic polymer additives for lightweight electromagnetic shielding. Aberdeen Proving Ground

(MD): Army Research Laboratory (US); 2015 Aug. Report No.: ARL-TR-7372.

List of Symbols, Abbreviations, and Acronyms

C/A	coarse acquisition
CERDEC	Communications-Electronics Research, Development and Engineering Center
C-ESPRIT	conjugated ESPRIT
CNT	carbon nanotube thread
CNT	carbon nanotube
CVD	chemical vapor deposition
CP&I	Command, Power & Integration Directorate
CRPA	controlled radiation/reception pattern antenna
CW	continuous wave
ESPRIT	estimation of signal parameters via rotational invariance techniques
GPS	global positioning system
HPBW	half power beamwidth
J/S	Jammer to signal
MUSIC	multiple signal classification
MWNT	multiwall carbon nanotube
PNT	position, navigation, and timing
RF	radio frequency
SINR	signal-to-interference-plus-noise-ratio

1   DEFENSE TECHNICAL
    (PDF)   INFORMATION CTR
                DTIC OCA

        2   DIRECTOR
    (PDF)   US ARMY RESEARCH LAB
                RDRL CIO LL
                IMAL HRA MAIL & RECORDS MGMT

        1   GOVT PRINTG OFC
    (PDF)   A MALHOTRA

        1   DIR USARL
    (PDF)   RDRL SER M
                    STEVEN D KELLER

INTENTIONALLY LEFT BLANK.